Journal Name

RSCPublishing

ARTICLE

Rhodanine-3-acetic acid and π-extended tetrathiafulvalene (*ex*TTF) based systems for Dye-Sensitized Solar Cells

Cite this: DOI: 10.1039/xoxxoooooo

Carlos Alberto Echeverry,[a] María Ángeles Herranz,[b] Alejandro Ortiz,[a] Braulio Insuasty*[a] and Nazario Martín*[b, c]

Received ooth January 2012,
Accepted ooth January 2012

DOI: 10.1039/xoxxoooooo

www.rsc.org/

We report here the synthesis, electrochemical and photophysical properties of a series of novel *ex*TTF-based organic dyes (**3** and **7a,b**) as well as their application in dye-sensitized solar cells (DSSCs). In the three designed dyes, the electron-donor *ex*TTF group is connected to the rhodanine-3-acetic acid electron-acceptor unit through vinyl or vinyl-thiophene spacers. The electrochemical studies showed that the energy gap between the LUMO level of the dyes and the TiO_2 conduction band decreases with the length of the conjugated system. As a consequence, the power conversion efficiencies of organic DSSCs fabricated with these dyes scale inversely to their light-harvesting ability.

Introduction

Dye-sensitized solar cells (DSSCs) have received widespread interest for transferring clean solar energy into electricity, becoming a new promising alternative to conventional solar cells.[1] In a typical DSSC device, light is absorbed by a monolayer of organic dye molecules anchored on the TiO_2 surface and then electrons are injected from the excited dye into the conduction band of the TiO_2, thus generating electric current.[2]

The interest in metal-free organic sensitizers has grown in the last years since they have high molar absorption coefficients, due to intramolecular π-π* transitions, and are easily modified due to relatively short synthetic routes.[3] In this regard, a great deal of research aiming at finding highly efficient and stable organic sensitizers has recently been performed and a wide number of new molecules involving triphenylamine,[4] porphyrin,[5] coumarin,[6] and perylene[7] derivates have been described as novel organic sensitizers.

The research on tetrathiafulvalene (TTF) and its π-extended derivatives (exTTFs) as electron donors in DSSCs has been limited if compared with the results considering the above mentioned electron-donor systems.[8] *ex*TTF-based organic dyes have showed an interesting behaviour and a moderated power conversion efficiency (η), due to a thermodynamically unfavourable dye-regeneration after electron-injection.[9] Although in recent results, dithiafulvene-based D-π-A[10] or annulated TTF-acceptor systems[11] have lead to very good power conversion efficiencies (6.5-8.3%).

Inspired by these results, in this paper we report the synthesis and characterization of three novel *ex*TTF-based dyes (Scheme 1), endowed with a rhodanine 3-acetic acid unit as the electron-acceptor and their further application as sensitizers in DSSCs. In our design, *ex*TTF-based aldehydes with different extension of the conjugation were connected to the active methylene of rhodanine 3-acetic acid through a Knoevenagel condensation. The prepared molecules (**3** and **7a**,**b**) were fully characterized by different spectroscopic methods and their optical, electrochemical and photophysical properties investigated considering experimental (absorption and emission spectroscopy, cyclic voltammetry) and theoretical (DFT calculations) methods. The experimental findings from the devices prepared reveal the strong impact that the modification of the π-conjugated bridge has on the photovoltaics performance of the DSSCs.

Results and discussion

Synthesis and characterization

As shown in Scheme 1, the target dyes **3** and **7a,b** were obtained by a Knoevenagel reaction of the aldehydes **2**[12] or **5a,b** and rhodanine 3-acetic acid **6** in moderate yields (49-55%). Aldehydes **5a,b** were prepared by Horner-Wadsworth-Emmons reaction of compound **2** with the corresponding diethyl 5-(1,3-dioxan-2-yl)-2-thienylmethyl phosphonate (**4**)[13] in good yields (77-83%). The red solids were fully characterized by NMR, IRTF, UV-Vis and MS spectrometry. The presence of the formyl group is clearly detected at 9.86 ppm in the ^{1}H

NMR, at 183.7-183.0 ppm in the ^{13}C NMR, as well as, by its stretching C=O band at 1658 cm^{-1} in the FTIR.

The target molecules **3** and **7a,b** exhibit a much lower solubility in common organic solvent than their precursors. As a general feature of these compounds, it is observed the signal corresponding to the methylene protons of rhodanine-3-acetic acid at high fields (δ = 4.10-4.80 ppm). The structures were also confirmed by HRMS MALDI-TOF mass spectrometry (see Experimental Section)

.

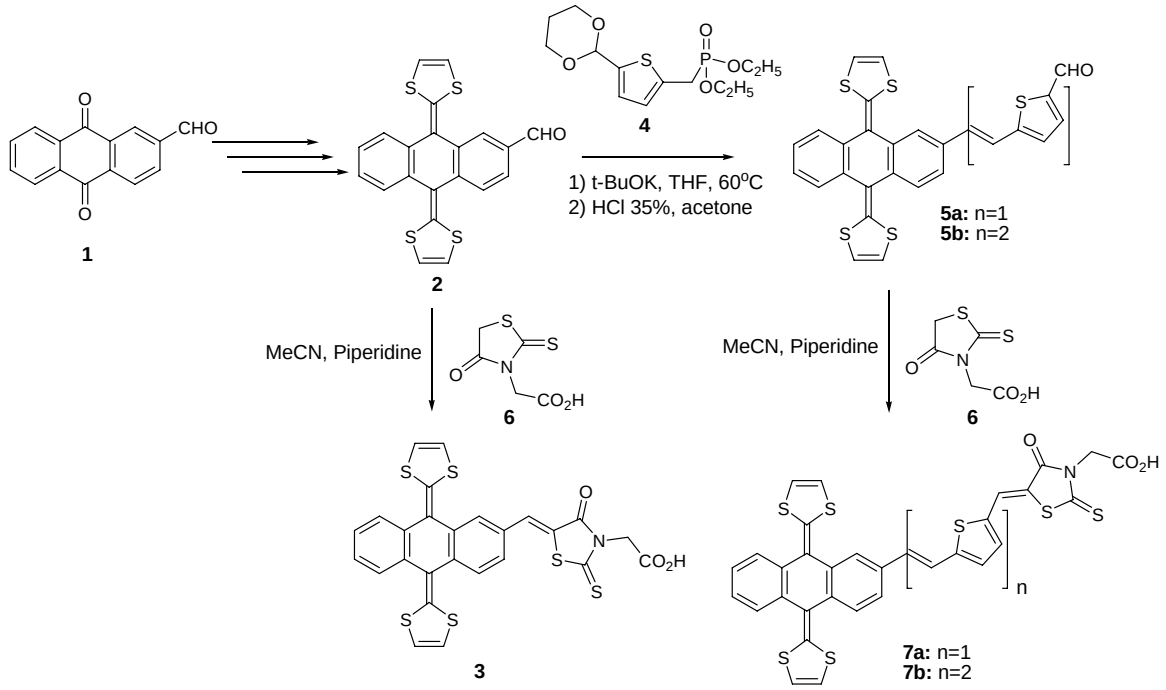

Scheme 1. Synthesis of the novel exTTF-based dyes **3** and **7a,b**.

Optical properties

The absorption spectra of *ex*TTF dyes (**3**, **7a,b**) in chloroform are shown in Fig. 1. The well-known absorptions of exTTF are observed in the 400−440 nm visible region.[14] Additionally, new absorption features are observed in the red part of the spectrum (starting from 500 nm). These low energy absorptions are assigned to charge transfer transitions involving the electron-donor exTTF and the electron-acceptor rhodanine 3-acetic acid moieties. Note that the above absorption bands are red-shifted and increase gradually their molar absorption coefficients (ε), ranging from 5449 to 28000 M^{-1} cm^{-1} (see Table 1), with the enhancement in the π-conjugation in the dyes.

Table 1. Maximum absorption and emission data of **3** and **7a,b** dyes

Dye	ε [$M^{-1}cm^{-1}$][a]	λ^{Abs}_{max} [nm][a]	λ^{Em}_{max} [nm][b]
3	5449	372	459
7a	6613	430	504
7b	28000	435	548

[a] Absorption spectra of dyes measured in chloroform with a concentration of 1×10^{-5} M; ε is the extinction coefficient at maximum absorption .[b] Emission spectra of dyes measured in chloroform with a concentration of 1×10^{-5} M.

The emission spectra for the new dyes **3**, **7a** and **7b** in solution were obtained by exciting at 370, 390 and 451 nm, respectively, which correspond to the wavelength of excitation where the compounds have the emission maximal. The emission spectra reflect the extended electronic conjugation on moving from **3** to **7a** and **7b** (Fig.1).[15] The emission bands of the dyes are structured with one distinct emission maximum and, shifted bathochromically with the increasing conjugation in the dyes without decreasing their fluorescence quantum yield.

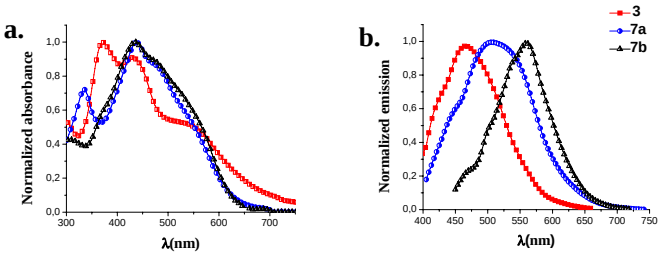

Fig. 1 Normalized absorption (a) and fluorescence emission spectra (b) of the new dyes based in *ex*-TTF (**3**, **7a-b**) dissolved in chloroform with a concentration of 1 x 10^{-5} M.

Electrochemical properties

The electrochemistry of *ex*TTF aldehydes (5**a,b**), target molecules (**3**, **7a,b**) and the reference 2-[9-(1,3-dithiol-2-

ylidene)anthracen-10(9H)-yilidene]-1,3-dithiole (*ex*TTF) were investigated by cyclic voltammetry in CH_3CN at room temperature. An $Ag/AgNO_3$ electrode was used as reference, a Pt wire as the counter electrode, and a glassy carbon was employed as working electrode (see Table 2). The *ex*TTF compounds exhibit a single two-electron chemically reversible oxidation process to form the dicationic state.[16] For all *ex*TTF compounds the oxidation potentials are very close (+43 to -15 mV) and both the anodic peak potential (E_{pa}) and the cathodic peak potential (E_{pc}) values are a function of the scan rate and the temperature, resulting in an electrochemically irreversible oxidation process, consequence of the coalescence of the first and second electron oxidations into a single two-electron wave. This oxidation process is accompanied by a drastic geometric change, from a highly distorted butterfly-like geometry in the neutral state to a planar, aromatic hydrocarbon skeleton in the dicationic state.[17] In the systems with the longest extended conjugation (**5b** and **7b**) and additional irreversible oxidation process, most probably due to the thiophenevinylene units, is observed at +850 and +781 mV, respectively. The *ex*TTF derivatives connected to rhodanine-3-acetic acid (**3** and **7a,b**) retain the anodic electrochemical pattern of *ex*TTF. However, the irreversible oxidation potentials are, in general, shifted to less negative values when compared to those of reference *ex*TTF (Table 2). On the reduction scan, very weak irreversible processes are detected at -1471 mV (**3**), -1379 mV (**7a**) and -1343 mV (**7b**). These reductions could be due to the conjugated system connected to the *ex*TTF and, not surprisingly, chain lengthening promotes a decrease in these reduction potentials.

Table 2 Electrochemical potentials [mV] of compounds **3**, **5a,b**, **7a,b** and reference *ex*TTF.

Dye	E^1_{ox} [a]	E^2_{ox} [a]	E^1_{red} [b]	E^2_{red} [b]
***ex*TTF**	-7(66)	--	--	--
5a	-15(44)	--	-1673(77)	-1981(55)
5b	+2(100)	+850	-1624(75)	-1787(75)
3	+27(44)	--	-1471[c]	--
7a	+43(96)	--	-1379[c]	--
7b	+22(76)	+781	-1343[c]	--

Values in parentheses correspond to the peak-to-peak separation. [a] E_{ox} are anodic peak potentials. [b] E_{red} are cathodic peak potentials. [c] Values obtained from square-wave voltammetry.

For device fabrication, the electronic levels of the HOMO (E_{ox}) and LUMO (E_{red}) should match the conduction band level of the semiconductor electrode and the iodine redox potential. The HOMO level ranging from -5.09 to -5.12 eV is more negative than the I^-/I_3 redox couple (-4,90 eV), which provides a a driving force for dye regeneration through the recapture of the injected electrons from I^- by the dye cation radical (Table 3). The energy gap between the LUMO level of the dyes and the conduction band edge of TiO_2 (-3.90 eV)[18] should be of at least 0.2 eV for an efficient electron injection. The E_{gap} ranging from 0.30 to 0.17 eV for the *ex*TTF-based dyes **3** and **7a,b** are very close to the limit driving forces. In the case of **7b**, this driving force is not sufficiently large to warrantee an effective electron injection.

Table 3 Orbital energy (eV) of the compounds **3** and **7a,b**.

Dye	$E_{0\text{-}0}$[eV]	E_{HOMO} [eV][a]	E_{LUMO} [eV][a]	E_{gap}[eV][b]
3	1.50	-5.10	-3.60	0.30
7a	1.42	-5.12	-3.70	0.20
7b	1.36	-5.09	-3.73	0.17

[a] Calculated with E_{HOMO}= -($E_{[ox\ vs.\ NHE]}$ + 4.75) eV and E_{LUMO}= -($E_{[red\ vs.\ NHE]}$ + 4.75) eV [b] E_{gap} is the energy gap between the E_{LUMO} of dye and the conduction band level of TiO_2 (-3.90 eV).

Electronic structure: theoretical calculations

Density functional theory (DFT) calculations were used to shed light on the electronic structure of the novel *ex*TTF-based organic dyes, using the Gaussian 09 suite of programs. The geometries of the final compounds were optimized using a B3LYP/6.31G(d, p) functional.[19]

Interestingly, the geometrical arrangement around the double-bond between the donor *ex*TTF and the thiophene ring consist in a *trans* disposition which shows a dihedral angle of approximately 180°. The compounds show a quasi-planar thiophene-rhodadine union, that should facilitate the electronic communication along the molecule through the thiophene wire. As expected, the ground state energies of the calculated dyes decrease when increasing the π-conjugation. We have also calculated the transition state energies by means of self-consistent field (SCF) method and conductor polarized continuum model (CPCM) in chloroform as solvent. The HOMO is mainly localized on the electron-donor moiety and the LUMO is mainly localized on the electron-acceptor unit of rhodanine-3-acetic acid with a small bridge contribution (Fig. 2).

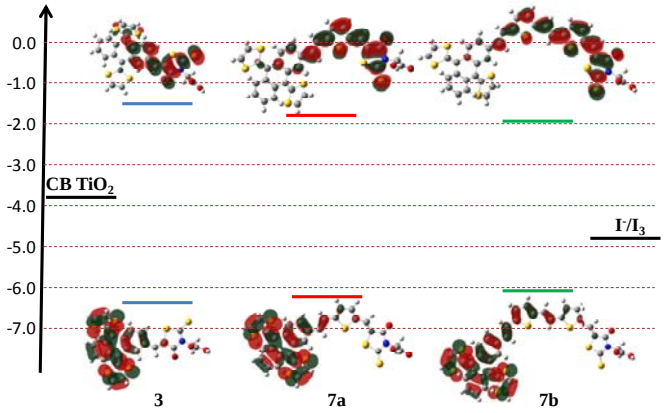

Fig. 2 Schematic energy diagram of synthetized dyes and the frontier molecular orbitals (HOMO and LUMO) calculated with DFT at a B3LYP/6-31G(d, p) level.

Interestingly, there is an overlap of HOMO and LUMO orbitals along the bridge, thus facilitating the electronic communication

between the donor and acceptor moieties. The orbital energy calculations showed that the novel *ex*TTF-based dyes have HOMO levels below the iodine redox couple level (-4.9 eV) to ensure the efficient regeneration of the oxidized dye by the triiodide in the electrolyte. The orbital LUMO levels are more positive than the conduction band level of the semiconductor (-3.9 eV) which, in principle, should be a sufficient driving force for the injection of the photoexcited electrons into the TiO_2 conduction band.

The lowest transitions for all compounds are listed in Table 4 in order to gain insight into the excited states of the dyes. The lowest transition for each dye is calculated to be at 2.78 eV (**3**), 2.61 eV (**7a**) and 2.39 eV (**7b**), corresponding to a charge-transfer excitation of the HOMO to the LUMO. The differences between absorption maximum from the theory and the experiments are related to the self-interaction error in TDDFT arising through the electron transfer in the extended charge-transfer state.[4b, 20]. In the case of dye **3**, can be observed that the band experimentally found at 2.21 eV (560 nm) seems to be composed by a transition with character of charge transfer with a oscillator strength of 0.5035 and the band at 2.88 eV (430 nm) appears to be principally composed by a transition of different composition from the HOMO-3 to the LUMO and the HOMO-1 to the LUMO, with energy values of 3.32 and 3.33 eV, respectively. The transition from the HOMO-1 to the LUMO has an oscillator strength calculated of 0.6215, showing that this transition is the more probable and corresponds to the λ^{Abs}_{max} detected at 372 nm (Table 1). Dye **7a** has a band experimentally found at 430 nm that appears to be principally composed by a transition HOMO-LUMO with an oscillator strength of 1.5663. The experimental band observed at 335 nm appears to be composed by three overlapping π–π^* transition of different composition from the HOMO-2 to the LUMO, the HOMO to the LUMO, the HOMO-4 to the LUMO and the HOMO to the LUMO+1, with values of energy of 3.06, 3.31 and 3.46 eV, respectively.

In the case of **7b**, calculations predict that part of the absorption tail observed around 520 nm is mostly due to a photoinduced charge-transfer transition between the donor exTTF moiety and the acceptor rhodanine-3-acetic acid unit, although no other contributions are clearly predicted.

Photovoltaic properties of DSSCs

The overall solar-to-electrical energy conversion efficiency (η) of DSSCs prepared with the synthesized dyes is calculated from the short-circuit photocurrent density (J_{sc}), the open-circuit voltage (V_{oc}), the fill factor of the cell (*FF*), and the intensity of the incident light (P_{in}) as follows:

$$\eta = \frac{J_{SC} V_{OC} FF}{P_{in}} \qquad (1)$$

Fig. 3 shows the corresponding photocurrent density-voltage (*J*-*V*) curves of the obtained DSSCs under simulated AM 1.5 solar irradiation at 100 mW cm^2. The photovoltaic data are summarized in Table 5.

Table 4. Calculated TD-DFT excitation energies (E), oscillator strengths (*f*), composition and character (CT= charge transfer).

Dyes	State	Composition	Character	E[eV,nm]	*f*
3	S1	H→L(0.65)	CT	2.78(445)	0.5035
	S2	H-3→L(0.57)	π-π^*	3.32(373)	0.0002
		H-3→L+1(0.30)	π-π^*		
		H-3→L+2(0.23)	π-π^*		
	S3	H-1→L(0.59)	CT	3.33(372)	0.6215
	S4	H-2→L(0.23)	π-π^*	3.54(351)	0.4936
		H→L+1(0.52)	π-π^*		
	S5	H-2→L(0.54)	π-π^*	3.82(325)	0.3373
		H-1→L(0.20)	CT		
		H→L+2(0.25)	π-π^*		
	S6	H→L+3(0.42)	π-π^*	3.96(313)	0.0810
7a	S1	H-1→L(0.36)	CT	2.61(476)	1.5663
		H→L(0.47)	CT		
	S2	H-2→L(0.26)	π-π^*	3.06(405)	0.0228
		H→L(0.39)	CT		
	S3	H-4→L(0.52)	π-π^*	3.31(374)	0.0001
	S4	H→L(0.24)	CT	3.46(358)	0.3039
		H→L+1(0.38)	CT		
	S5	H-3→L(0.17)	π-π^*	3.63(341)	0.3941
		H-2→L(0.42)	CT		
		H-1→L+2(0.15)	π-π^*		
	S6	H→L+3(0.48)	π-π^*	3.87(320)	0.1414
7b	S1	H-1→L (0.50)	CT	2.39(519)	2.0667
		H→L (0.40)	CT		
	S2	H-3→L(0.18)	π-π^*	3.06(405)	0.2438
		H-1→L (0.31)	π-π^*		
		H→L+1 (0.41)	π-π^*		
	S3	H-5→L(0.47)	π-π^*	3.33(3.73)	0.0015
	S4	H-3→L(0.31)	π-π^*	3.38(367)	0.8561
		H→L+1 (0.48)	π-π^*		
	S5	H-1→L (0.31)	CT	3.47(358)	0.3880
		H→L+2 (0.39)	π-π^*		
	S6	H-2→L(0.18)	CT	3.71(334)	0.0073

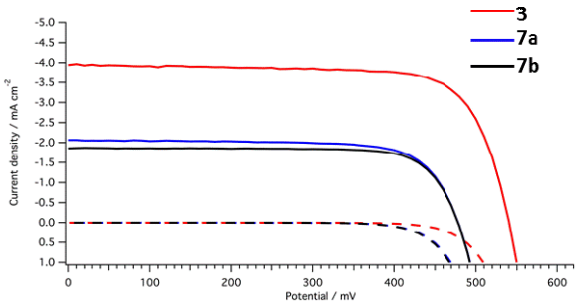

Fig. 3 Current-voltage characteristics for the DSSCs based on **3** and **7a,b**.

The concentration of dye employed for the preparation of devices was the same in the three cases, $3x10^{-4}$ M. Films were dipped in the respective dye for 15 hours. The photovoltaic energy conversion efficiency data show the order of **7b** < **7a** < **3**. The DSSC based on **3** shows better comprehensive properties with an open circuit voltage of 0.539 V, a short circuit photocurrent density of 3.943 mA cm^{-2}, and a fill factor of 0.745, corresponding to an overall light to electricity conversion efficiency of 1.59%.

Table 5. Photovoltaic performance of DSSCs sensitized with the as-synthesized dyes.

Dyes	J_{sc} [mA cm^{-2}]	V_{OC} [V]	FF	η%
3	3.943	0.539	0.745	1.59
7a	2.062	0.477	0.728	0.72
7b	1.857	0.477	0.767	0.68

[a] The concentration of all dyes was the same ($3x10^{-4}$ M) and commercially available Degussa (P25) was used for making photo-anodes. Films were dipped in the respective dyes for 15 hours.

In comparison with the reported DSSCs based on exTTF,[9] the present devices show a lower photocurrent generation. The J_{sc} of the DSSCs increases in the order of **7b <7a <3**, although the absorption spectrum is wider in the dyes with thiophene as a bridge, the injection efficiency and regeneration of the oxidized dye is affected, because the driving force for all dyes is very low. Most probably the quite close separation of the HOMO level of the dyes (-5.09 to -5.12 eV) and the oxidation potential for the I^-/I_3 redox couple with an energy of -4.9 eV, results in a lower driving force for regeneration of the oxidized dye by iodide in the electrolyte.[21, 22] In addition, the low values for the J_{sc} could also be attributed to the lack of conjugation with the acceptor, since there is not a good coupling of the energy levels between the pigment and the TiO_2. The energy gap between the LUMO level of the dyes and the conduction band edge of TiO_2 are very close to the limit of driving forces ($E_{gap} \approx 0.2$ eV),[6, 23] in the case of **7b** (E_{gap}=0.17 eV), this is obviously not sufficiently large for effective electron injection leaving a low conversion efficiency (η= 0.68%).

Conclusions

We have prepared and fully characterized three novel *ex*TTF-based dyes for DSSC applications. From density functional theory (DFT) calculations and frontier orbital analysis, it is evident that the HOMO is mainly localized on the electron-donor moiety and the LUMO is mainly localized on the electron-acceptor unit of rhodanine-3-acetic acid with a small bridge contribution, showing a pronounced push-pull effect. Unfortunately, the low gaps between the HOMO of the dyes and the I^-/I_3 redox couple in one side and, the LUMO levels of the dyes and the conduction band of TiO_2 in the other, prevent a functional operation of the DSSCs. Among the investigated dyes, the device made with **3** exhibits the best performance, with an overall power conversion efficiency of a 1.59%.

Experimental section

General. All solvents were dried according to standard procedures. Reagents were used as purchased. All air-sensitive reactions were carried out under argon atmosphere. Flash chromatography was performed using silica gel (Merck, Kieselgel 60, 230-240 mesh or Scharlau 60, 230-240 mesh). Analytical thin layer chromatography (TLC) was performed using aluminum coated Merck Kieselgel60 F254 plates. Melting points were determined on a Sanyo Gallenkamp apparatus. NMR spectra were recorded on a Bruker Avance 300 (^{1}H: 300 MHz; ^{13}C: 75 MHz) and BrukerAvance 700 (^{1}H: 700 MHz; ^{13}C: 176 MHz) spectrometer at 298 K using partially deuterated solvents as internal standards. Coupling constants (*J*) are denoted in Hz and chemical shifts (δ) in ppm. Multiplicities are denoted as follows: s = singlet, d = doublet, t = triplet, m = multiplet, br = broad. FT-IR spectra were recorded on a Bruker Tensor 27 (ATR device) spectrometer. UV-Vis spectra were recorded on a Varian Cary 50 spectrophotometer using $CHCl_3$ as solvent. Matrix Assisted Laser Desorption Ionization (coupled to a Time-Of-Flight analyzer) experiments (MALDI-TOF) were recorded on a HP1100MSD spectrometer and a Bruker REFLEX spectrometer respectively.

Electrochemistry. Cyclic voltammetry was performed using an AutolabPGStat 30. A glassy carbon working electrode (Metrohm 6.0804.010) was used after being polished with alumina (0.3 μm) for 1 min, and platinum wire was used as counter electrode. An $Ag/AgNO_3$ electrode was used as a reference. Tetra-*n*-butylammonium hexafluorophosphate ($TBAPF_6$) (0.1 M) was used as supporting electrolyte and dry tetrahydrofuran as solvent. The samples were purged with argon prior to measurement. The scan rate was 100 mV/s.

Cell fabrication:

Photoanode. FTO glass (TEC7) was cleaned and an under layer of TiO_2 was deposited by heating the substrates for 30 min at 70 ˚C in an aqueous solution of $TiCl_4$. Then an 8-μm layer of transparent TiO_2 was screen-printed. The paste used for this layer contained nanoparticles of 18 nm diameters. A scattering layer formed by 400 nm Ø nanoparticles (5 μm thick)

was deposited on the transparent layer. The whole structure was calcined up to 500 ˚C.

Sensitization. Solutions containing 0.3 mM of each dye in THF/EtOH (1:4) mixture were prepared. Prior the immersion in the solutions, the photoanodes were heated to 450 ˚C and cooled down to 80˚C. The sensitization process lasted 15 hours.

Cell assembly. Twice platinized (drop casting of a solution of 8 mM hexachloroplatinic acid in *n*-propanol followed by heating to 410˚C for 15 min) FTO glass pieces with pre-drilled holes served as counter electrodes. They were sealed with dried sensitized photoanodes by hot-melt polymer rings (Surlyn, Dupont – 25µm thickness). Electrolyte (1 M dimethylimidazolium iodide, 0.03 M I_2, 0.1 M guanidinium thiocyanate, 0.5 M *t*-butylpyridine, 0.05 M lithium iodide in MeCN/*s*-BuCN 85:15 v/v) was driven into the device via a pre-drilled hole using a vacuum pump. The hole was sealed with a polymer and a covering glass.

Measurement: A 450 W xenon light source (Oriel, USA) was used to characterize the solar cells. The spectral output of the lamp was matched in the region of 350–750 nm with the aid of a Schott K113 Tempax sunlight filter (Präzisions Glas & Optik GmbH, Germany) so as to reduce the mismatch between the simulated and true solar spectra to less than 2%. The current–voltage characteristics of the cell under these conditions were obtained by applying external potential bias to the cell and measuring the generated photocurrent with a Keithley model 2400 digital source meter (Keithley, USA). A similar data acquisition system was used to control the incident photon-to-current conversion efficiency (IPCE) measurement. Under computer control, light from a 300 W xenon lamp (ILC Technology, USA) was focused through a Gemini-180 double monochromator (Jobin Yvon Ltd., UK) onto the photovoltaic cell under test. The devices were masked to attain an illuminated active area of 0.159 cm^2.

Compound 5a

To solution of aldehyde **2**[12] (100 mg, 0.24 mmol) and phosphonate **4**[13] (78.4 mg, 0.24 mmol) in dry THF (20 mL) was added a solution of *t*-BuOK (30.1 mg,0.27 mmol) in dry THF (10 mL) at 60 ^oC under argon atmosphere, and then the mixture was stirred for 2 h at the same temperature. The mixture was washed with water, the aqueous layer was extracted with dichloromethane and the combined organic parts were dried over Na_2SO_4. After removal of the solvents under reduced pressure, 20 mL of acetone and 3 mL of a solution of HCl 35% were added, stirring 2h. The mixture was washed with water, the aqueous layer was extracted with chloroform and the combined organic parts were dried over Na_2SO_4, filtered and evaporated. The residue was purified by flash column chromatography (silica gel, CH_2Cl_2/hexane, 2/1) to afford **5a** as a red solid (95 mg, 77%). ^1H NMR ($CDCl_3$, 300 MHz) δ 9.87 (s, 1H) 7.84 (d, *J*=1.37 Hz, 1H) 7.66-7.75 (m, 4H) 7.40 (dd, *J*=8.10, 1.65 Hz, 1H) 7.29-7.34 (m, 2H) 7.21 (d, *J*=6.72 Hz, 2H) 7.14-7.19 (m, 1H) 6.29-6.36 (m, 4H) ppm. ^{13}C NMR ($CDCl_3$, 75 MHz) δ 183.0, 153.0, 141.9, 137.7, 137.1, 136.7, 136.4, 136.3, 135.6, 135.6, 133.8, 133.1, 127.0, 126.5, 125.9, 125.3, 125.2, 123.6, 122.2, 122.1, 121.1, 117.8, 117.7, 117.4 ppm. FT-IR ν: 653, 755, 807, 961, 1045, 1094, 1225, 1266, 1448, 1508, 1548, 1659, 2857, 2925, 3065 cm^{-1}. Melting point, 173-177 ^oC. UV-Vis ($CHCl_3$), λ_{max}: 359, 412 nm; HRMS (MALDI): calcd. for $C_{27}H_{16}OS_5$ 515.9807; found 515.9811 [M^+].

Compound 5b

To a solution of compound **5a** (100 mg, 0.19 mmol) and phosphonate **4**[13] (61.0 mg, 0.19 mmol) in dry THF (20 mL) was added a solution of *t*-BuOK (23.4 mg,0.21 mmol) in dry THF (10 mL) at 60 ^oC under argon atmosphere, and then the mixture was stirred for 2 h to the same temperature. The mixture was washed with water, the aqueous layer was extracted with dichloromethane and the combined organic parts were dried over Na_2SO_4. After removal of the solvents under reduced pressure, 20 mL of acetone and 3 mL of a solution of HCl 35% were added, stirring 2h. The mixture was washed with water, the aqueous layer was extracted with chloroform and the combined organic parts were dried over Na_2SO_4, filtered and evaporated. The residue was purified by flash column chromatography (silica gel, CH_2Cl_2/hexane, 2/1) to afford **5b** as a red solid (99.6 mg, 83%). ^1H NMR ($CDCl_3$, 300 MHz) δ 9.86 (s, 1H), 7.82 (d, *J*=1.51 Hz, 1H), 7.71 (dd, *J*=5.83, 3.09 Hz, 2H), 7.65-7.69 (m, 2H), 7.38 (dd, *J*=8.03, 1.58 Hz, 1H), 7.29–7.33 (m, 2H), 7.26 (d, *J*=2.33 Hz, 1H), 7.20 (d, *J*=2.47 Hz, 1H), 7.13 (d, *J*=3.98 Hz, 1H), 7.04-7.07 (m, 1H), 6.99-7.03 (m, 2H), 6.96 (d, *J*=6.72 Hz, 1H), 6.33 (s, 4H) ppm. ^{13}C NMR (*DMSO-d_6*, 75 MHz) δ 183.7, 151.1, 143.2, 141.1, 140.2, 139.0, 137.0, 136.9, 135.2, 134.6, 134.3, 134.2, 130.1, 128.4, 128.3, 127.7, 126.2, 125.7, 125.1, 124.7, 124.4, 122.6, 122.1, 120.4, 118.3, 118.2, 118.1 ppm. FT-IR ν: 643, 719, 771, 1159, 1266, 1377, 1459, 1504, 1593, 1657, 1736, 2857, 2924 cm^{-1}. Melting point, 191-197 ^oC desc. UV-Vis ($CHCl_3$), λ_{max}: 438 nm; HRMS (MALDI): calcd. for $C_{33}H_{20}OS_6$ 623.9841; found 623.9833 [M^+].

Compound 3

A solution of aldehyde **2**[12] (100 mg, 0.24 mmol) and rhodanine 3-acetic acid **6** (51.5 mg, 0.27 mmol) in MeCN (20 mL) was refluxed for 12 h in the presence of piperidine (0.2 mL). Afterwards, the solvents were evaporated and the mixture was then dissolved in dichlorometane and washed with an aqueous solution of hydrochloric acid 1M, the combined organic parts were dried over Na_2SO_4, filtered and evaporated. The residue was purified by flash column chromatography (silica gel, ethyl acetate/MeOH, 10/1) to afford **3** as a black solid (78.3 mg, 55%). ^1H NMR (*DMSO-d_6*, 700 MHz) δ: 13.55 (m, 1H), 7.95 (s, 1H), 7.85 (m, 2H), 7.72 (d, *J*=7.00 Hz, 1H), 7.70-7.71 (m, 2H), 7.37-7.41 (m, 2H), 6.80-6.88 (m, 4H), 4.76 (s, 2H) ppm. ^{13}C NMR (*DMSO-d_6*, 176 MHz) δ: 193.2, 167.8, 166.9, 140.5, 138.6, 137.7, 136.0, 134.8, 134.7, 133.7, 130.6, 130.4, 127.0, 127.0, 126.2, 125.4, 125.1, 121.7, 120.2, 120.1, 119.1, 119.1, 118.9, 118.5, 55.4, 45.7 ppm. FT-IR ν: 649, 749, 805, 1057, 1109, 1197, 1280, 1325, 1366, 1408, 1453, 1504, 1547, 1585, 1714, 2936, 3068, 3402 cm^{-1}. Melting point, 302-306 ^oC. UV-

Vis ($CHCl_3$), λ_{max}: 371, 430, 560 nm; HRMS (MALDI): calcd. for $C_{26}H_{15}NO_3S_6$ 580.9378; found 579.9303 [M^+-1].

Compound 7a

A solution of compound **5a** (100 mg, 0.19 mmol) and rhodanine 3-acetic acid 6 (40.7 mg, 0.21 mmol) in MeCN (20 mL) was refluxed for 12 h in the presence of piperidine (0.2 mL). The solvents were evaporated. The mixture was then dissolved in dichlorometane and washed with aqueous solution of hydrochloric acid 1M, the combined organic parts were dried over Na_2SO_4, filtered and evaporated. The residue was purified by flash column chromatography (silica gel, ethyl acetate/MeOH, 10/1) to afford **7a** as a black solid (66.7 mg, 50%). ^{1}H NMR (*DMSO-d*$_6$, 300 MHz) δ: 8.17 (s, 1H), 7.94 (s, 1H), 7.79-7.81 (m, 1H), 7.65-7.70 (m, 4H), 7.63 (d, *J*=14.00 Hz, 1H), 7.48 (d, *J*=14.00 Hz, 1H), 7.3-7.39 (m, 3H), 6.82-6.77 (m, 4H) 4.74 (s, 2H) ppm. ^{13}C NMR (*DMSO-d*$_6$, 176 MHz) δ: 192.3, 137.8, 137.7, 135.79, 135.2, 135.0, 134.5, 129.4, 126.8, 125.6, 125.3, 125.2, 123.5, 121.9, 120.9, 120.8, 118.9, 118.8, 118.7, 118.6, 56.5 ppm. FT-IR ν: 650, 749, 804, 897, 947, 1052, 1110, 1200, 1323, 1366, 1438, 1507, 1579, 1649, 1714, 2933, 3065 cm^{-1}. Melting point, > 350 ºC desc. UV-Vis ($CHCl_3$), λ_{max}: 335, 438 nm; HRMS (MALDI): calcd. for $C_{32}H_{19}NO_3S_7$ 688,9413; found 688,9390 [M^+].

Compound 7b

A solution of compound **5b** (100 mg, 0.16 mmol) and rhodanine 3-acetic acid 6 (36.7 mg, 0.19 mmol) in MeCN (20 mL) was refluxed for 12 h in the presence of piperidine (0.2 mL). The solvents were evaporated. The mixture was then dissolved in dichlorometane and washed with aqueous solution of hydrochloric acid 1M, the combined organic parts were dried over Na_2SO_4, filtered and evaporated. The residue was purified by flash column chromatography (silica gel, ethyl acetate/MeOH, 10/1) to afford **7b** as a black solid (62.6 mg, 49%). ^{1}H NMR (*DMSO-d*$_6$, 300 MHz) δ: 7.95 (s, 1H), 7.78 (s, 1H), 7.65 (d, *J*=4.24 Hz, 1H), 7.56-7.63 (m, 3H), 7.46 - 7.54 (m, 1H), 7.43 (d, *J*=6.28 Hz, 1H), 7.38 (s, 1H), 7.35 (d, *J*=3.65 Hz, 1H), 7.28-7.32 (m, 2H), 7.24 (d, *J*=3.22 Hz, 1H), 7.17 (m, 2 H), 6.96 (d, *J*=16.22 Hz, 1H), 6.67-6.75 (m, 4H), 4.18 (s, 2H) ppm. ^{13}C NMR (*DMSO-d*$_6$, 176 MHz) δ: 192.1,167.0, 166.5, 150.6, 143.1, 141.2, 137.5, 137.5, 137.3, 136.9, 135.7, 135.1, 134.8, 134.6, 130.3, 129.3, 129.0, 128.6, 126.7, 125.6, 125.4, 125.2, 125.0, 124.9, 123.0, 122.7, 121.0, 120.9, 120.9, 120.5, 118.8, 118.7, 118.5, 63.5, 49.1 ppm. FT-IR ν: 640, 750, 800, 941, 1052, 1108, 1198, 1321, 1368, 1414, 1455, 1510, 1577, 1646, 1707, 1929, 3391 cm^{-1}.Melting point, > 350 ºC desc. UV-Vis ($CHCl_3$), λ_{max}: 435 nm; HRMS (MALDI): calcd. for $C_{38}H_{23}NO_3S_8$ 796.9447; found 795.9401 [M^+-1].

Acknowledgements

This work has been supported by COLCIENCIAS (Colombia) and the Universidad del Valle (Colombia). Financial support from the European Research Council ERC-2012-ADG_20120216 (Chirallcarbon), MINECO of Spain (CTQ2011-24652) and CAM (grant number MADRISOLAR-2 S2009/PPQ-1533) is greatly appreciated.

Notes and references

[a] Departamento de Química, Facultad de Ciencias Naturales y Exactas, Universidad del Valle, A.A. 25360 Cali, Colombia
Fax:+57-2-3393248
E-mail:braulio.insuasty@correounivalle.edu.co
[b] Departamento de Química Orgánica, Facultad de Química, Universidad Complutense, 28040 Madrid, Spain.
Fax:+34-91-3944103
E-mail:nazmar@quim.ucm.es.
[c] IMDEA-Nanoscience, Campus de Cantoblanco, Universidad Autónoma de Madrid, 28049 Madrid, Spain.

1 (a) A. Hagfeldt, G. Boschloo, L. Sun, L. Kloo and H. Pettersson, *Chem. Rev.*, 2010, **110**, 6595; (b) Z. Ning and H. Tian, *Chem. Commun.*, 2009, 5483.

2 (a) M. Grätzel, *Inorg. Chem.,* 2005, **44**, 6841; (b) T. Le Bahers, T. Pauporté, G. Scalmani, C. Adamo and I. Ciofini, *Phys. Chem. Chem. Phys.*, 2009, **11**, 11276.

3 A. Mishra, M. K. Fischer and P. Bäuerle, *Angew. Chem. Int. Ed.*, 2009, **48**, 2474.

4 (a) C.-H. Yang, H.-L. Chen, Y.-Y. Chuang, C.-G. Wu, C.-P. Chen, S.-H. Liao and T.-L. Wang, *Journal of Power Sources*, 2009, **188**, 627; (b) W. Xu, B. Peng, J. Chen, M. Liang and F. Cai, *J. Phys. Chem. C*, 2008, **112**, 874; (c) Y. Liang, B. Peng, J. Chen, *J. Phys. Chem. C,* 2010, **114**, 10992; (d) A. Dualeh, F. De Angelis, S. Fantacci, T. Moehl, C. Yi, F. Kessler, E. Baranoff, M. Nazzeruddin, M. Grätzel, *J. Phys. Chem. C,* 2012, **116**, 1572; (e) A. Tigreros, V. Dhas, A. Ortiz, B. Insuasty, N. Martín, L. Echegoyen, *Solar Energy Materials & Solar Cells*, 2014, **121**, 6162.

5 (a) A. Yella, H-W. Lee, H. Tsao, C. Yi, A. Chandiran, M. Nazeeruddin, E. Diau, C. Yeh, S. Zakeeruddin, M. Grätzel, *Science,* 2011, **334**, 629; (b) C. W. Lee, H.P. Lu, C. M. Lang, Y. M. Huang, Y. M., Liang, W. N, Yen, Y. C. Liu, Y. S. Lin, E. Diau and C. Y. Yeh, *Chem. Eur. J.,* 2009, **15**, 1403; (c) S. Mathew, A. Yella, P. Gao, R. Humphry-Baker, B. F. E. Curchod, N. Ashari-Astani, I. Tavernelli, U. Rothlisberger, Md. K. Nazaaruddin and M. Grätzel, *Nature Chem.,* 2014, **6**, 242.

6 K. Hara, T. Sato, R. Katoh, A. Furube, Y. Ohga, A. Shinpo, S. Suga, K. Sayama, H. Sugihara and H. Arakawa, *J. Phys. Chem. B,* 2003, **107**, 597.

7 (a) T. Edvinsson, C. Li, N. Pschirer, J. Shöneboom, F. Eickemeyer, R. Sens, G. Boschloo, A. Hermann, K. Müllen and A. Hagfeldt, *J. Phys. Chem. C,* 2007, **111**, 15137; (b) D. K. Panda, F. S. Goodson, S. Ray, R. Lowell and S. Saha, *Chem. Commun.,*, 2012, **48**, 8775; (c) C. Huang, S. Barlow, S. Marder, *J. Org. Chem.,* 2011, **76**, 2386.

8 Y. Geng, F. Pop, Ch. Yi, N. Avarvari, M. Grätzel, S. Decurtins and S.-X. Liu, *New. J. Chem.,* 2014, **38**, 3269.

9 S. Wenger, P.-A. Bouit, Q. Chen, J. Teuscher, D. D. Censo, R. Humphry-Baker, J.-E. Moser, J. L. Delgado, N. Martín, S. M. Zakeeruddin and M. Grätzel, *J. Am. Chem. Soc.*, 2010, **132**, 5164.

10 K. Guo, K. Yan, X. Lu, Y. Qiu, Z. Liu, J. Sun, F. Yan, W. Guo and Sh. Yang, *Org. Lett.,* 2012, **14**, 2214.

11 A. Amacher, Ch. Yi, J. Yang, M. P. Bircher, Y. Fu, M. Cascella, M. Grätzel, S. Decurtins and S.-X. Liu, *Chem. Commun.,* 2014, **50**, 6540.

12 N. Martín, I. Pérez, L. Sánchez and C. Seoane, *J. Org. Chem.* 1997, **62**, 5690.
13 C. Zhang, A. W. Harper and L. R. Dalton, *Synth. Commun.,* 2001, **31**, 1361.
14 (a) P. A. Bouit, C. Villegas, J. L. Delgado, P. M. Viruela, R. Pou-Amérigo, E. Ortí and N. Martín, *Org. Lett.,* 2011, **13**, 604; (b) R. García, M. A. Herranz, M. R. Torres, P.-A. Bouit, J. L. Delgado, J. Calbo, P. M. Viruela, E. Ortí and N. Martín, *J. Org. Chem.,* 2012, **77**, 10707.
15 I. Osken, A. S. Gundogan, E. Tekin, M. S Eroglu and T. Ozturk, *Macromolecules*, 2013, **46**, 9202.
16 (a) S. G. Liu, I. Pérez, N. Martín and L. Echegoyen*, J. Org. Chem.,* 2000, **65**, 9092; b) I. Pérez, S. G. Liu, N. Martín and L. Echegoyen, *J.Org. Chem.,* 2000, **65**, 3796.
17 M. A. Herranz, L. Yu, N. Martín and L. Echegoyen, *J.Org. Chem.,* 2003, **68**, 8379.
18 L. Yu, K. Fan, T. Duan, X. Chen, R. Li and T. Peng, *ACS Sustainable Chem. Eng.*, 2014, **2**, 718.
19 N. Martsinovich, A. Troisi, *Energy Enviro. Sci.*, 2011, **4**, 4473.
20 A. Dreuw, M. Head-Gordon, *J. Am. Chem. Soc.*, 2004, **126**, 4007.
21 P. Qin, X. Yang, R. Chen, L. Sun, T. Marinado, T. Edvinsson, G. Boschloo, A. Hagfeldt, A. *J. Phys. Chem. C,* 2007, **111,** 1853.
22 C. A. Echeverry, A. Insuasty, M. Á. Herranz, A. Ortíz, R. Cotta, V. Dhas, L. Echegoyen, B. Insuasty and N. Martín, *Dyes and Pigments*, 2014, **107**, 9.
23 M. Liang, W. Xu, F. Cai, P. Chen, B. Peng, J. Chen and Z. Li, *J. Phys. Chem. C*, 2007, **111**, 4465.

